Preparation of bi-modified amphoteric oligochitosan derivatives and electrochemical evaluation on anticorrosion performances

Huixin Zhang,[1] Dongdong Wang,[1] Xiuhong Jin,[2] Tingru Yang,[1] Xiaoli Shen[2]

[1]School of Chemistry and Chemical Engineering, Hebei University of Technology, Tianjin 300130, China
[2]China National Offshore Oil Corporations, Tianjin Chemical Research and Design Institute, Tianjin 300130, China
Correspondence to: H. Zhang (E-mail: zhanghuixin@hebut.edu.cn)

ABSTRACT: Four bi-modified amphoteric oligochitosan derivatives were synthesized chemically using quaternization, sulfonation, and carboxylation. The anticorrosion characteristics and mechanism of anticorrosion of these four oligochitosan derivatives on Q235 steel in 1.0 mol/L HCl solution were studied by potentiodynamic polarization and electrochemical impedance spectroscopy at constant temperature. The results suggest that these derivatives are hybrid corrosion inhibitors in which anodic inhibition predominates following the mechanism of adsorption film formation on the surface of the metal. They all have their own optimal dosages for anti-corrosion application. Their inhibiting efficiencies are closely related to the nature and the amount of heteroatoms in their molecules. © 2014 Wiley Periodicals, Inc. J. Appl. Polym. Sci. **2015**, *132*, 41714.

INTRODUCTION

Chitosan is the *N*-deacetylated product of chitin, which is a natural macromolecular compound obtained from the exoskeleton of shellfish and insects, with a large number of hydroxyl and amino groups. Although the chitosan is naturally abundantly available from chitin, its applications in industries are limited to smaller extent because of its poor solubility and reactivity and poor performance in applications.[1–4] Therefore, the degradation techniques and further modification of chitosan have drawn great attention. Nowadays, the main methods of degradation of chitosan are enzymatic decomposition, chemical decomposition such as acid hydrolyzation and oxidative degradation, and physical treatment. The oxidative degradation technique is one of the chemical decomposition techniques. It is very popular because it has the advantages of less pollution, rapid reaction rate, and high yield compared with the other degradation techniques. The oxidants in the oxidative degradation include $KMnO_4$, O_3, MnO_2, ferrate, H_2O_2, OsO_4, Cu_2O, and so on. Among them, H_2O_2 oxidative degradation is widely used because of low cost, availability, and good operability.[5–8] Also, the reaction products of H_2O_2 are water and radicals that will be consumed in attacking the β-D-(1,4)-glucosidic linkages of chitosan. However, the formation of radical groups is inefficient and the quality of degradation product is not good, with wide distribution in molecular weight (MW) and big fluctua-

tion in average MW when H_2O_2 alone is used[8]; thus, researchers have combined other degradation technologies with H_2O_2. Because of the thermal and special effects of microwave, the oxidative degradation method assisted with microwave radiaion will achieve further improvement in reaction speed and yield, facilitate operation, and economize energy and materials. Thus, the degradation of chitosan by microwave/H_2O_2 hybrid process will be more efficient, easier to handle, and more eco-friendly. In this study, the oligochitosan (OC) was degraded using this new technique. The resultant product was good, with narrow MW distribution and stable in a setting average MW.

The modification of chitosan is mainly carried out by grafting and crosslinking through quaternization, sulfonation, carboxylation, and acylation. The resulting chitosan derivatives may have better water solubility, mechanical strength, stability, or chelating ability, with metal ions as adsorbent, flocculant, or chelating agent.[9–11] Also, chitosan has good physiological efficacy, such as boosting metabolism and immunity.[9,10] The OC in this study was modified with *cis*-epoxysuccinic acid, 2,3-oxiranemethane sulfonic acid sodium salt, 1-acrylamido-2-methylpropane sulfonic acid (AMPS), or chloroacetic acid at first and then with 2,3-epoxypropyl trimethyl ammonium chloride (EPTAC). The resulted bi-modified amphoteric OC derivatives were not only better in solubility and reactivity than the raw chitosan and OC, but also were nontoxic and non-phosphorus. They are

Additional Supporting Information may be found in the online version of this article.

environment-friendly, meeting the requirements for green water chemicals.

The corrosion is a common damage in various industrial water systems and industrial practices. The corrosion over the surface of facilities and configuration will cause great financial losses and serious security problems unless proper measures are adopted. When the metal is exposed to acidic or chlorine-rich medium, the corrosion will be worse, as hydrogen and chloride ions damage the oxidation film and accelerate the dissolution of metal.[12,13] The application of corrosion inhibitors is one of the most effective and practical methods for protecting metals and utilities against corrosion.[13] According to their action sites, anodic corrosion inhibitors, cathodic corrosion inhibitors, and hybrid corrosion inhibitors are considered for industrial and scientific applications. With the increasing environmental awareness, the exploitation and use of corrosion inhibitors have become a demanding work, and environmental friendly corrosion inhibitors are becoming more and more popular.[14] A mass of environmental friendly corrosion inhibitors, including amino acids, synthetic polymers, natural products, and some of the heterocyclic compounds have been reported, which have high corrosion inhibition efficiency, low toxicity for humans and environment, and so on.[15–18] Zaferani et al.[19] summarized a series of eco-friendly products as corrosion inhibitors for metals in acid pickling processes, which indicated that eco-friendly corrosion inhibitors can play a major role instead of the toxic synthetic ones. Li et al.[4] reported that aminothiourea-modified chitosan worked as corrosion inhibitor in 2% HAc with corrosion inhibition efficiency of 90% at a dosage of 60 mg/L. Fekry[3] research indicated that acetyl thiourea chitosan can be used as corrosion inhibitor for mild steel in 0.5 mol/L sulfuric acid medium. Its inhibition efficiency reached 94.5% for 0.76 mmol/L dosage of acetyl thiourea chitosan. Quraishi[20] reported that the corrosion inhibitor of 4-salicylideneamino-3-hydrazino-5-mercapto-1,2,4-triazole was 19.15%–72.34% in 15% HCl for N80 steel, when the dosage was 250–1000 mg/L. Although the environment-friendly corrosion inhibitors have obtained some valuable achievements, they also have some disadvantages. For example, the exact mechanisms governing corrosion on various metals are not clear. Also, the high cost according to their availability, processing method, and production volume[19] and the disunity of the evaluation criteria because of diversity in evaluation methods, test parameters, and so on confine their development and applications in industries. Concerning the structures and characters of bi-modified amphoteric OC derivatives, they are qualified as environment-friendly corrosion inhibitors. There are some reports on the use of OC derivatives as corrosion inhibitor for metals, but few of them discuss the studies in interaction mechanisms and structure–function relationships.[3,4,11] To achieve high corrosion inhibition efficiency and to study the relationship between inhibition behaviors and functional groups, the OC was modified by combining heteroatom groups, and the derivatives were evaluated on anti-corrosion performances by electrochemical methods and scanning electron microscopy (SEM) in this study.

In the field of corrosion, the film formation is considered as the major mechanism of corrosion inhibition. The film forming on the surface of metal can prevent corrosion through obstructing the exchange of charge and substance, restraining electrode reaction, and so on. Oxidation, precipitation, adsorption, and electrochemical inhibition are considered to be main mechanisms of film formation. Most of the organic corrosion inhibitors are inclined to adsorption film formation mechanism. The corrosion inhibition efficiency of organic compounds is related to their adsorption properties, and capability of these molecules depends mainly on certain physicochemical properties of the inhibitor molecules such as functional groups, steric factors, aromaticity, electron densities at the donor atoms, orbital characters of donating electrons, and electronic configuration of the molecules.[19–22] Adsorption can be described by physisorption and chemisorption. As the inhibitors adsorb on the surface of metal, they can retard the corrosion reaction. In the other hand, the inhibitors can militate with metal surface or corrosion products, separating the metal surface from corrosive medium. Most commercial acid-inhibitors are organic compounds containing heteroatoms such as nitrogen, oxygen, sulfur, and phosphorous atoms. This indicates that heteroatom groups play an important role in corrosion inhibition. This is why the OC derivatives are synthesized with different heteroatom groups and thus studied to clarify their antiscaling mechanisms and structure–function relationships between the corrosion behaviors and the natures of heteroatom functional groups.

The corrosion characteristics and inhibition mechanism of inhibitors can be studied by static weight-loss method, rotary coupon method, and electrochemical technologies, which include potentiodynamic polarization (PDP), linear polarization resistance method, potentiostatic-galvanostatic measurement, electrochemical noise technology, electrochemical impedance spectroscopy (EIS), linear polarization resistance measurement, and so on. Among these methods, the EIS and PDP are widely used in the research of inhibition mechanism and electrochemical characterization for corrosion inhibitors because these measurements are reliable, reproducible, and easy to be handled. They can present direct results.

In this study, four bi-modified amphoteric OC derivatives with different heteroatoms were synthesized successfully, and their inhibitory performances and inhibition mechanism were studied mainly by PDP and EIS. Also, the close relationships between corrosion inhibition efficiency and chemistry, such as steric effect, hydrophilicity, surface charges, and kinds and amount of heteroatom groups are discussed. They proved to be efficient hybrid corrosion inhibitors of Q235 steel even in 1 mol/L HCl solution, and the mechanism of adsorption film formation on the surface of the metal is suggested.

EXPERIMENTAL

Materials and Facilities

Chitosan (degree of deacetylation >95%, viscosity average MW of 350 kDa) was purchased from Jinan Haidebei Marine Bioengineering Co. Ltd. (Shandong, China). Hydrogen peroxide (AR) and microwave experiment instrument (MG08S-28) were used in the degradation of chitosan. EPTAC (AR), epichlorohydrin (AR), chloroacetic acid (AR), and ammonium persulfate (AR) were used in the preparation of OC derivatives. The nuclear magnetic resonance (NMR) spectrometer (Bruker AV 400) and

the infrared spectrometer (Bruker, TENSOR 27) were applied in the structure confirmation of OC and four OC derivatives. All the electrochemical experiments were carried out using VersaStudio integrated test system (UPH-I-20L).

Synthesis of OC Derivatives

Degradation of Chitosan. The OC in this study was obtained by degrading chitosan in microwave/H_2O_2 system. Briefly, 2 g of chitosan was added to acetic acid. Then H_2O_2 (30 mL, 4%) was added to the mixture. The reaction mixture was stirred continuously for a setting period of time. The duration, the temperature, and the microwave power for the degradation were set according to the expectations of MW. The typical values were 6 min, 70°C, and 220 W, respectively, when the desired MW was 6000 or thereabouts with a narrow distribution. Then, the OC was got after filtration and drying.[23] The degradation experiment was carried out several times to verify the accuracy of the degradation conditions. The structure of OC was confirmed by Fourier transform infrared (FT-IR) spectra.

Anionic Group Modifications of OC. The anionic group modifications of OC (AOC) were carried out as follows: Organic acids or their salts and OC were added to distilled water. Each mixture was stirred at certain temperature for a period time shown in Figure 1. Each mixture was precipitated by acetone–alcohol (1 : 1, v/v) mixture and then centrifuged to obtain sediments. The anion-modified products of OC were obtained after filtration and dried at 40°C–50°C.[23–26]

Cationic Group Modifications of AOC. The derivatives from cationic group modifications of AOC (CAOC) were perpared by stirring EPTAC and the products from AOC at 85°C for10 h in alkaline solution. Each reaction mixture was adjusted to neutral pH, and then precipitated in acetone–alcohol mixture for 12 h. The modified products were obtained from the sediments after drying at 40°C–50°C.[23–26]

cis-Epoxysuccinic acid, 2,3-oxiranemethane sulfonic acid sodium salt, 1-acrylamido-2-methylpropanesulfonic acid, and chloroacetic acid were used for AOC. EPTAC was used for CAOC. The CAOC products were *N*,O-(hydroxyl-succinyl)-*N*-[chloro-2′-hydroxyl-3′-(*N′*,*N′*,*N′*-trialkyl-)propylamino]-OC (SU-QAOC), *N*,O-(hydroxyl propyl sulfonyl)-*N*-[chloro-2′-hydroxyl-3′-(*N′*,*N′*,*N′*-trialkyl-) propylamino]-OC (PS-QAOC), *N*,O-(2-methyl-2-acrylamido-propylsulfonyl)-*N*-[chloro-2′-hydroxyl-3′-(*N′*,*N′*,*N′*-trialkyl-) propylamino]-OC (AMPS-QAOC), and *N*,O-carboxymethyl-*N*-[chloro-2′-hydroxyl-3′-(*N′*,*N′*,*N′*-trialkyl-) propylamino]-OC (CM-QAOC).The synthetic route is shown in Figure 1.

Electrochemical Evaluation Methodology

Preparation of Electrodes. Pt electrode and saturated calomel electrode were used as auxiliary electrode and reference electrode, respectively. A coupon of Q235 steel was used as working electrode, having a layer of coating of epoxy resin adhesive. A part of 1.0 cm^2 section-area of the coupon was left bare and uncovered to be exposed to the HCl solution. Before application, the working electrode was polished by a series of SiC abrasive paper from 400 grits down to 1000 grits until it became even, smooth, and free of nicks, scratches, and pocking marks. Then, it was washed with

distilled water and absolute ethanol and finally dried. Before experiment, the working electrode must be immersed in the test solution until the potential remained stable. All electrochemical tests were carried out at constant temperature and accomplished over a three-electrode system.

Acquisition of Polarization Curves. Polarization curves were recorded at a constant sweep rate of 0.5 mV/s over a scanning range from −300 to +300 mV with respect to the open circuit potential. The analysis of polarization curves was accomplished by VersaStudio software, and the corrosion inhibition efficiency [η (%)] was calculated by eq. (1).[27]

$$\eta(\%) = \frac{i_{corr}^0 - i_{corr}}{i_{corr}^0}\% \qquad (1)$$

where, i_{corr}^0 and i_{corr} are corrosion current densities in the absence and presence of inhibitors, respectively.

EIS Measurements. The experiments were carried out in a frequency range from 100 kHz to 5000 mHz with amplitude of 1.0 mV peak-to-peak using AC signals at open circuit potential. The equivalent circuit was matched by ZSimpWin. The corrosion inhibition efficiency [η (%)] and double-layer capacitance (C) were calculated by eqs. (2) and (3), respectively.

$$\eta(\%) = \frac{R_{ct} - R_{ct}^0}{R_{ct}}\% \qquad (2)$$

$$C = \frac{1}{\omega R_{ct}} \qquad (3)$$

where, R_{ct}^0 and R_{ct} are the charge transfer resistance values in the absence and presence of inhibitors, respectively, and ω is the frequency at apex on Nyquist plot.

RESULTS AND DISCUSSION

### Degradation of Chitosan and Synthesis of Bi-Modified Amphoteric OC Derivatives

The yield of soluable OC from microwave/H_2O_2 degradation was 62%. The MW was 5900–6200, and the polydispersity index was only 1.21–1.24, which indicated that the OC had narrow MW distribution. In Ref. [8, H_2O_2 of 30% was used alone for chitosan degradation at 70°C within 30 min, and the degradation ratio was 43%.[8] However, the data of MW and polydispersity index were not mentioned in Ref. [8, which is the common situation for most reports on chitosan degradation.

Four OC derivatives were synthesised successfully, verified by spectral data (in the following section), and the yields for SU-QAOC, PS-QAOC, AMPS-QAOC, and CM-QAOC were 55, 57, 75, and 68%, respectively. The conversion percentages of OC for SU-QAOC, PS-QAOC, AMPS-QAOC, and CM-QAOC were 67, 68, 76, and 70%, respectively.

The FT-IR spectra for OC and four OC derivatives are shown in Figure 2. Their FT-IR and ^{1}H-NMR data are shown in the Supporting Information file.

Analysis of Polarization Curves

The polarization curves of the four OC derivatives (SU-QAOC, PS-QAOC, AMPS-QAOC, and CM-QAOC) and their starting OC in different dosages are shown in Figure 3. The electrochemical parameters such as corrosion potential (E_{corr}),
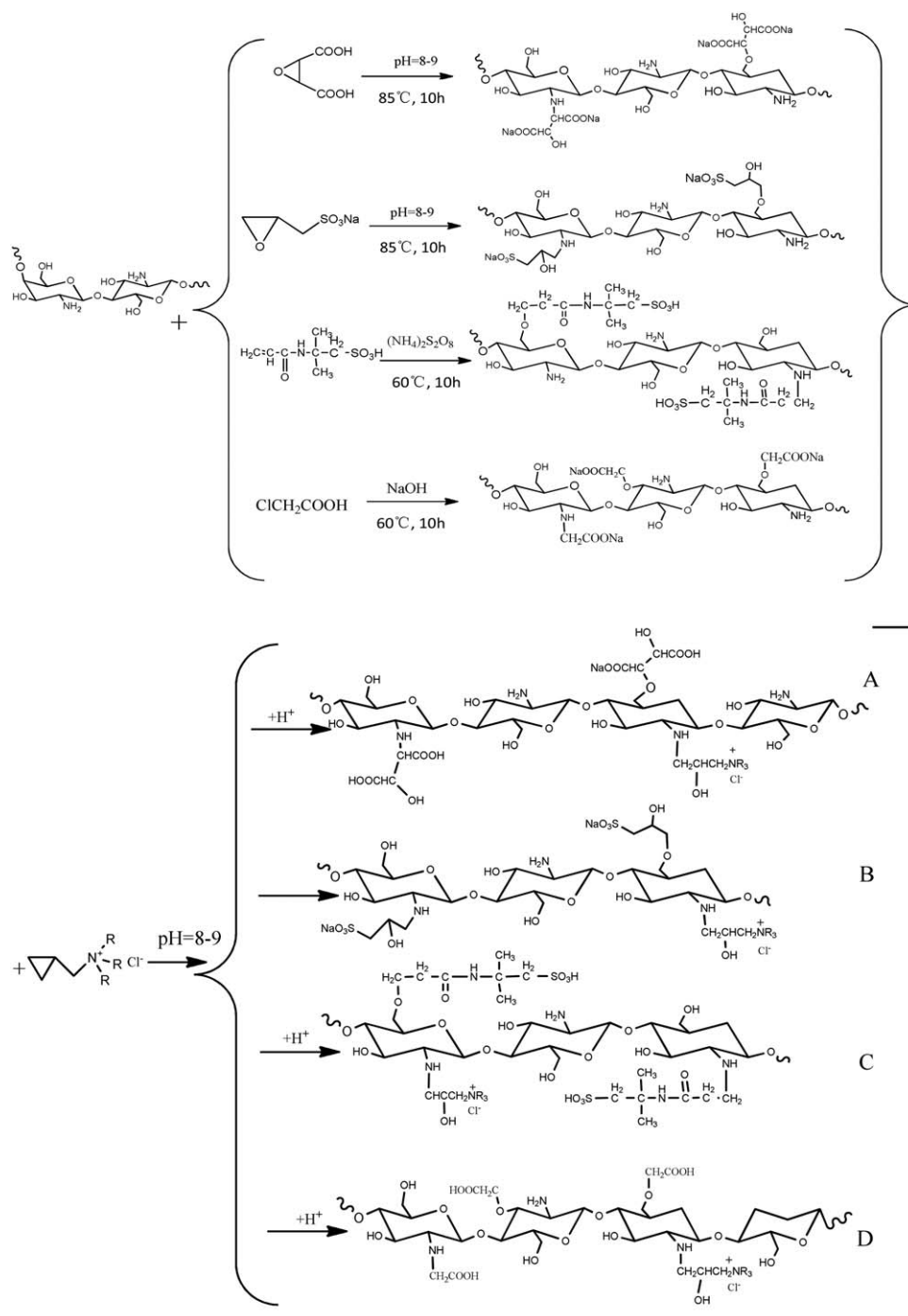
Figure 1. The synthetic route for the four bi-modified amphoteric OC derivatives. A: SU-QAOC; B: PS-QAOC; C: AMPS-QAOC; and D: CM-QAOC.

cathodic and anodic Tafel slopes (β_c and β_a), corrosion current density (i_{corr}), and corrosion inhibition efficiency [η (%)] are listed in Table I.

From Figure 3 it can be seen that the polarization curves of the four OC derivatives and OC showed no obvious differences compared with the polarization curves of blank in the shape. This indicates that the electrode reactions were not changed with the addition of derivatives and OC.

Compared with the blank, the corrosion inhibition efficiencies and E_{corr} of all derivatives and OC elevated, which indicated that the reaction activation energy barrier rose and the anodic reaction was restrained within the presence of any of the four ones and OC. So the protection of the derivative inhibitors over the steel coupon was enhanced and the corrosion inhibitors worked, resulting in negative catalysis.[27,28] Normally, the anodic inhibitor makes the E_{corr} to elevate more than 85 mV, the
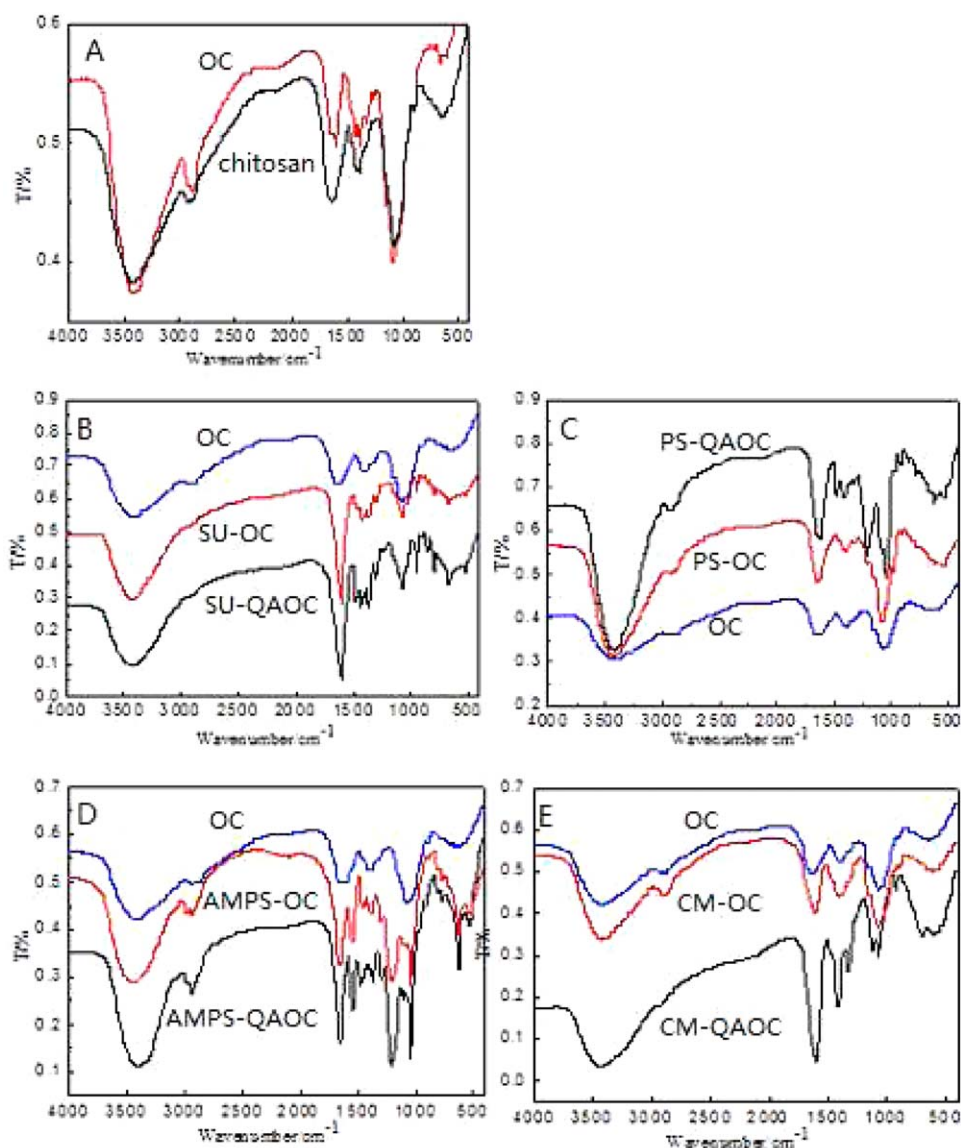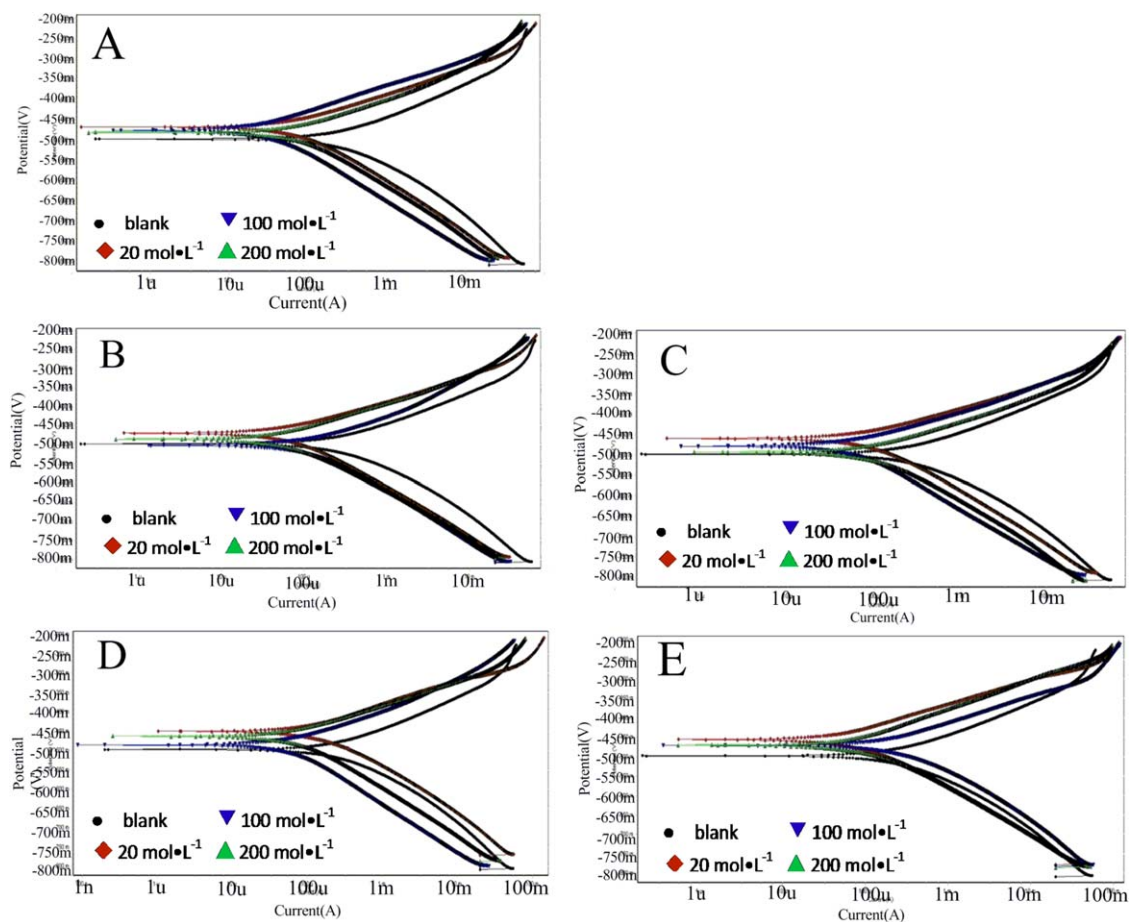
Figure 2. The FT-IR spectra of A: OC, B: SU-QAOC, C: PS-QAOC, D: AMPS-QAOC, and E: CM-QAOC. [Color figure can be viewed in the online issue, which is available at wileyonlinelibrary.com.]

cathodic inhibitor makes it to decline, and the hybrid inhibitor makes it not to elevate more than 85 mV. From the results in Table I, it can be seen that the corrosion potentials went up, but the elevated values did not exceed 85 mV. So, the four OC derivatives are hybrid inhibitors.

As the Tafel slope was considered, the higher the slope is, the weaker the impact of potential shift on corrosion rate will be. The results in Table I and Figure 3 showed that the anodic slopes of the four derivatives decreased more sharply than the cathode slopes did. It indicated that the decrease in anodic reaction rates were more obvious than the corresponding cathodic ones. From all the information above, it can be concluded that the four derivatives are hybrid inhibitors with predominant anodic inhibition.[29,30]

The corrosion current density (i_{corr}) reflects how easily or difficultly electrode reaction occurs. The corrosion reaction will be easier to occur with higher i_{corr}, so the corrosion inhibition effi-

ciency will be lower, and *vice versa*.[31,32] From Table I, it can be seen that the corrosion current densities of SU-QAOC, AMPS-QAOC, and CM-QAOC decreased and then elevated with the increasing dosages of the inhibitors; so, the corrosion inhibition efficiencies elevated and then decreased. The corrosion inhibition efficiencies reach to a peak with a dosage of only 100 mg/L; hence, that is 87.36%, 71.26%, or 68.63%, respectively, for SU-QAOC, AMPS-QAOC, or CM-QAOC. However, the efficiency of OC is 58.74% with the same dose. The above three QAOCs are superior to OC, and SU-QAOC makes the others pale beside it. The comparison with some eco-friendly and common corrosion inhibitors are shown in Table II.[3,4,11,13,27] It can be seen that SU-QAOC has better corrosion efficiency than some of the common corrosion inhibitors. The reasons lay in the fact that the coverage of the adsorption film will increase usually with the increase in inhibitor dosage. So the inhibition efficiencies of SU-QAOC, AMPS-QAOC, and CM-QAOC

Figure 3. Polarization curves with different dosages of inhibitor. A: OC; B: SU-QAOC; C: PS-QAOC; D: APMS-QAOC; and E: CM-QAOC. [Color figure can be viewed in the online issue, which is available at wileyonlinelibrary.com.]

Table I. Fitting Data and Corrosion Inhibition Efficiency of Polarization Curve

Dosage (mg/L)	E_{corr} ($\times 10^3$) (V)	β_a ($\times 10^3$) (V·dec^{-1})	β_c ($\times 10^3$) (V·dec^{-1})	i_{corr} ($\times 10^3$) (A cm^{-2})	η (%)
SU-QAOC-20	−468.76	68.544	−119.73	70.613	68.20
SU-QAOC-100	−477.17	70.098	−114.13	28.070	87.36
SU-QAOC-200	−481.43	76.856	−124.48	81.997	63.07
PS-QAOC-20	−470.06	70.008	−122.53	65.766	70.38
PS-QAOC-100	−475.56	75.796	−123.84	102.46	53.86
PS-QAOC-200	−485.50	78.280	−118.50	62.340	71.93
AMPS-QAOC-20	−459.38	70.059	−126.72	90.913	59.60
AMPS-QAOC-100	−478.67	73.316	−128.58	63.826	71.26
AMPS-QAOC-200	−492.76	77.385	−130.25	114.44	48.46
CM-QAOC-20	−450.73	73.512	−119.15	142.09	36.01
CM-QAOC-100	−485.96	82.919	−131.06	69.648	68.63
CM-QAOC-200	−463.36	66.598	−120.10	71.760	67.68
OC-20	−471.67	79.536	−127.72	211.51	4.750
OC-100	−450.73	83.245	−114.15	91.612	58.74
OC-200	−456.24	72.515	−111.67	65.478	70.51
Blank	−498.09	84.945	−121.12	222.05	–

Table II. Comparison of Eco-friendly, Common Corrosion Inhibitors and QAOCs

Inhibitor	Dosage	Medium	Metal	Test technique	η^a (%)	Ref. no.
Acetyl thiourea chitosan	0.78 mmol/L	0.5 mol/L H_2SO_4	Mild steel	PDP, EIS, SEM	94.5	3
Aminothiourea-modified chitosan	60 mg/L	2% HAc	Steel	PDP	90	4
1-(2-Ethylamino)-2-methylimidazolidine	10–100 mg/L	0.5 mol/L HCl	N80 steel	a^b, EIS	39–70	26
Benzimidazole	2 mol/L	1 mol/L HCl	Mild steel	b^c, PDP	60	13
4-Salicylideneamino-3-hydrazino-5-mercapto-1,2,4-triazole	250–1000 mg/L	15% HCl	N80 steel	a^b	19–72	39
CM-chitosan	200 mg/L	1 mol/L HCl	Q235 steel	PDP, EIS	93	11
SU-QAOC	100 mg/L	1 mol/L HCl	Q235 steel	PDP, EIS, SEM	87.36	This study
PS-QAOC	200 mg/L	1 mol/L HCl	Q235 steel	PDP, EIS, SEM	71.93	This study
AMPS-QAOC	100 mg/L	1 mol/L HCl	Q235 steel	PDP, EIS, SEM	71.26	This study
CM-QAOC	100 mg/L	1 mol/L HCl	Q235 steel	PDP, EIS, SEM	68.63	This study

[a] Corrosion inhibition efficiency.
[b] Linear sweep voltammetry.
[c] Weight loss.

increased when the dosages were raised to 100 mg/L from 20 mg/L. Then, when the dosages of the three QAOCs were 200 mg/L, the chelates of the corrosion products with the inhibitors may fall off from the surface of steel and the coating integrality would been destroyed, as a result the corrosion inhibition efficiencies decreased.

The anti-corrosion efficiency of PS-QAOC decreased and then increased along with its increasing dosage from 20 mg/L to 200 mg/L. The reason may be that chlorine ion can adsorb over the surface of steel when the coverage of the adsorption film is low at the dosage of 100 mg/L, so the metal can be chlorinated and dissolve into water. In this way, the transfer resistance will decrease and the steel will be corroded. The coverage will improve once the dosage of PS-QAOC increases from 100 mg/L to 200 mg/L, and the transfer can be hindered consequently. As a result, the corrosion inhibition efficiency of PS-QAOC elevated.[33] Further explanations are provided in the Analysis of Inhibition Mechanism section.

Analysis of EIS
The equivalent circuit fitted by ZSimpWin software is shown in Figure 4. The Nyquist plots and Bode plots for different dosages of SU-QAOC, PS-QAOC, AMPS-QAOC, and CM-QAOC are shown in Figures 5 and 6, respectively.
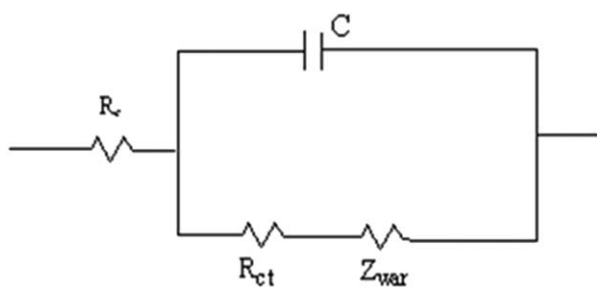

Figure 4. Equivalent circuit of bi-modified amphoteric OC derivatives in 1 mol/L HCl solution.

Some parameters such as solution resistance (R_s), the charge transfer resistance values in the absence and presence of inhibitors (R_{ct}^0 and R_{ct}), the frequency at apex on Nyquist plot (ω), the double-layer capacitance (C), and corrosion inhibition efficiency [η (%)] are listed in Table III.

The electrical equivalent circuit that is generally used to simulate the electrochemical behavior can be interpreted in Figure 4. Z_{war} indicates a Warburg tail that appears in the Nyquist plots with the existence of corrosion inhibitors. The low frequency part of Nyquist plot corresponds to the relaxation process of the impedance nature, which shows the adsorption film properties of steel surface. The high frequency part of Nyquist plot corresponds to the AC signal response of double layer capacitance which shows the charge and discharge relaxation process of the loop formed by C and R_{ct}.

From Figures 5 and 6, it can be seen that the impedance spectra changed to irregular capacitive reactance arc when different QAOC inhibitors were added into solution of 1 mol/L HCl. The feeble raised borders at the right end of the Nyquist plots indicate that there are blurry Warburg impedance arc and capacitive reactance arc in the lower frequency part. The presence of Warburg impedance arc suggests that diffusion process is an important step of electrode process. However, only one distinct time constant can be identified. These indicate that the electrode reaction and even corrosion process of Q235 steel are mainly controlled by charge transfer in 1 mol/L HCl solution.[34,35] The semicircle diameter in the Nyquist plot corresponds to the charge transfer resistance. The bigger the charge transfer resistance, the better the protection of the adsorbing film will be, and so the inhibitor will be more efficient. According to Figure 5 and Table III, the charge transfer resistances of QAOCs increase obviously and double-layer capacitances of QAOCs decrease in contrast to the solution without inhibitor. The increase in the charge transfer resistance is due to the formation of adsorption film when the inhibitors were added into the HCl solution. The reciprocal of the double layer capacitance is in
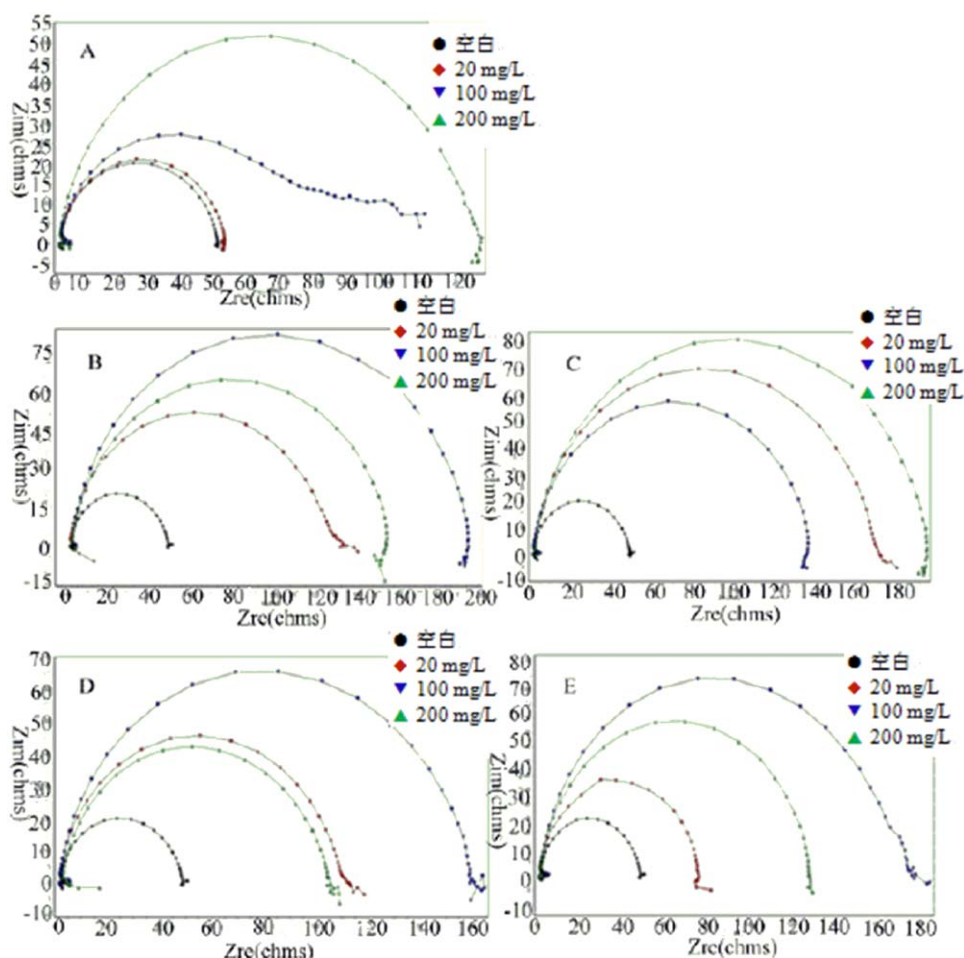
Figure 5. Nyquist plots of different concentrations. A: OC; B: SU-QAOC; C: PS-QAOC; D: APMS-QAOC; and E: CM-QAOC. [Color figure can be viewed in the online issue, which is available at wileyonlinelibrary.com.]

direct proportion to the thickness of the adsorption film on the steel. As the capacitance of the double-layer declines, the thickness of the protective film on the surface of steel increases. It can be speculated that the inhibitor adsorbs on the steel replacing the water molecular, which has higher dielectric constant and smaller size to form a close adsorbing film and mainly hinder the transfer of charge. As a result, the charge transfer resistance value increases, which is consistent with the experiment results. Furthermore, the decrease in i_{corr} with the addition of inhibitors is an evidence of the adsorption film. Therefore, the inhibition mechanism is the typical adsorption-film mechanism.

As can be seen from Table III, the charge transfer resistances of SU-QAOC, AMPS-QAOC, or CM-QAOC increase and then reduce with the increase in inhibitor dosages; the corrosion inhibition efficiencies also follow the same pattern. This is similar to the results of the polarization curves. The highest corrosion inhibition efficiencies of SU-QAOC, AMPS-QAOC, and CM-QAOC were 75.34%, 70.66%, and 73.52%, respectively, as the dosage comes to 100 mg/L, whereas the highest efficiencies of PS-QAOC and OC were 75.61% and 62.65% at a dosage of 200 mg/L. In conclusion, the QAOCs give much better corrosion inhibition than do the OC. The inhibition efficiency of

SU-QAOC is higher than that of the three others; so, it outdoes the other derivatives.

Analysis of Inhibition Mechanism

In the case of corrosion to steel in the chlorine-rich medium, the active anions (such as chlorine) adsorb on the surface of metal and combine with it resulting in negative catalysis. So the metal is dissolved and transferred as cation into solution. The anions tend to adsorb on the defect sites. The impact of anions on corrosion varies depending on the nature of anion ions, metal, and its corrosion products. With the entrance of anions, the oxidation film has more charge carriers; also the anions can enter the metal dissolution reaction. As a result, corrosion pits emerge on the metal surface, and serves as active center for corrosion.[30]

Within the molecules of the four OC derivatives, there are many hydroxyl, amino, and carboxyl groups, and many electronegative atoms like O, N, and S. They have a lone pair of electrons, which can chelate the metal and form complex. A wide spread of protective film will result on the surface of metal hindering the corrosion mainly through preventing the charge of ions. The differences among the four derivatives are mainly due to the different function groups that can influence the corrosion
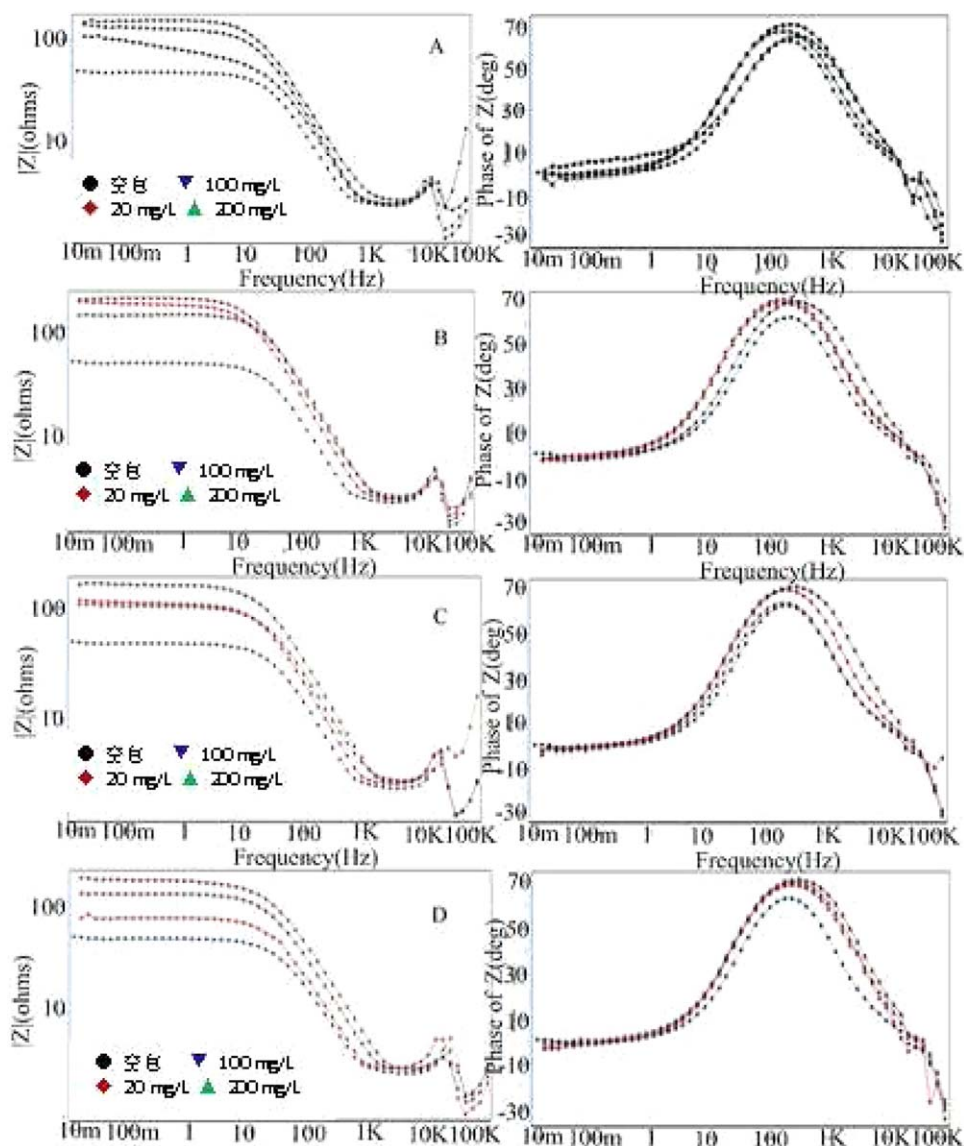
Figure 6. Bode plots of different dosages. A: SU-QAOC; B: PS-QAOC; C: APMS-QAOC; and D: CM-QAOC. [Color figure can be viewed in the online issue, which is available at wileyonlinelibrary.com.]

inhibition properties. SU-QAOC has the most hydroxyl, amino, and carboxyl groups among the QAOCs. So it has the highest adsorption activity. Furthermore, hydrogen bonding can enhance the adsorption film, making it stable and integral. These are the reasons why SU-QAOC has the best corrosion inhibition.[35–39] Concerning other derivatives, PS-QAOC has more hydroxyl than AMPS-QAOC and CM-QAOC. Furthermore, the sulfonic group has better coordination ability than carboxyl. So, PS-QAOC has better corrosion inhibition efficiency than AMPS-QAOC and AMPS-QAOC has better corrosion inhibition efficiency than CM-QAOC. The study suggested that all the four modified OCs are hybrid inhibitors, with predominating anodic inhibition, which indicates that the modification does not change the electrode reaction, whereas the dissolution of metal is restrained by formation of adsorption film. The schematic diagram is shown in Figure 7.

The quaternized modification of OC can increase the solubility, and this has facilitated its application in hindering corrosion. But their molecules have more charges, which can impact the formation of adsorption film due to electrostatic repulsion. Furthermore, the amphoteric OC derivatives can chelate with corrosion products and they can lead to the destruction of protection film. Therefore, the corrosion inhibition efficiency may reduce when the dosage of inhibitors increases. Because of these reasons, the i_{corr} rose up when the dosages elevate to 200 mg/L. Besides, the chlorine ion does some damages to the protective film, and thus the corrosion inhibition will take a turn for the worse.[19]

For PS-QAOC, its surface charges are a little more than that of other QAOCs, and the volume of its function groups are smaller than SU-QAOC and AMPS-QAOC; so, the electrostatic repulsion can play a greater role.[40,41] Besides, the strong

**Table III.** Fitting Data and Corrosion Inhibition Efficiency from EIS

Dosage (mg/L)	R_s [$\Omega \cdot cm^2$]	R_{ct} ($\Omega \cdot cm^2$)	Ω (Hz)	C ($\times 10^4$) ($F \cdot cm^2$)	η (%)
SU-QAOC-20	2.9200	126.93	17.780	4.4310	63.56
SU-QAOC-100	1.9600	187.53	17.780	2.2490	75.34
SU-QAOC-200	2.3800	149.59	23.710	2.8190	69.24
PS-QAOC-20	2.8000	165.04	13.330	4.5450	71.98
PS-QAOC-100	1.7300	131.60	23.740	3.2010	64.49
PS-QAOC-200	2.3300	189.62	17.780	2.9670	75.61
AMPS-QAOC-20	1.5000	107.72	17.780	5.2210	57.06
AMPS-QAOC-100	1.5300	157.66	17.780	3.5670	70.66
AMPS-QAOC-200	3.1100	100.53	31.620	3.1460	54.00
CM-QAOC-20	1.0700	73.179	31.620	4.3320	36.80
CM-QAOC-100	1.6700	174.63	23.710	2.4150	73.52
CM-QAOC-200	1.4000	126.55	23.710	3.3330	63.45
OC-20	1.2900	48.093	42.160	4.9320	3.830
OC-100	1.4400	89.017	23.710	4.7380	48.04
OC-200	1.1800	123.95	17.780	4.5380	62.65
Blank	1.0292	46.250	31.620	6.8380	–

hydrophilicity and polarity of function groups lead to the strong interaction between the adsorption film and aqueous phase. The combination of all these reasons may cause desorption of PS-QAOC and lead to the damage of adsorption film. So, the inhibition efficiency of PS-QAOC decreased when the dosage reached 100 mg/L, whereas it occurred at a dosage of 200 mg/L for the three others. When the dosage of PS-QAOC reached 200 mg/L, the inhibitor can restrain some parts of the film falling off the metal surface on account of the interaction of inhibitor molecules. Furthermore, the interaction of the function groups with aqueous phase and metal surface can also explain the behavior of PS-QAOC. These are the reasons why PS-QAOC

shows different anticorrosion behavior among the four derivatives. However, the protecting films of other derivatives were not damaged seriously when the dosage reached 100 mg/L because of the reasons above. So, their inhibition efficiencies increased further from the dosage of 100 mg/L to 200 mg/L. These reasons can explain why the four QAOCs have their own optimal dosages in corrosion inhibition.

Analysis of SEM Images

To give more obvious differentiations between modified OC derivatives and OC, SEM analysis was conducted. Figure 8 illustrates the SEM figures for the samples at their own optimal
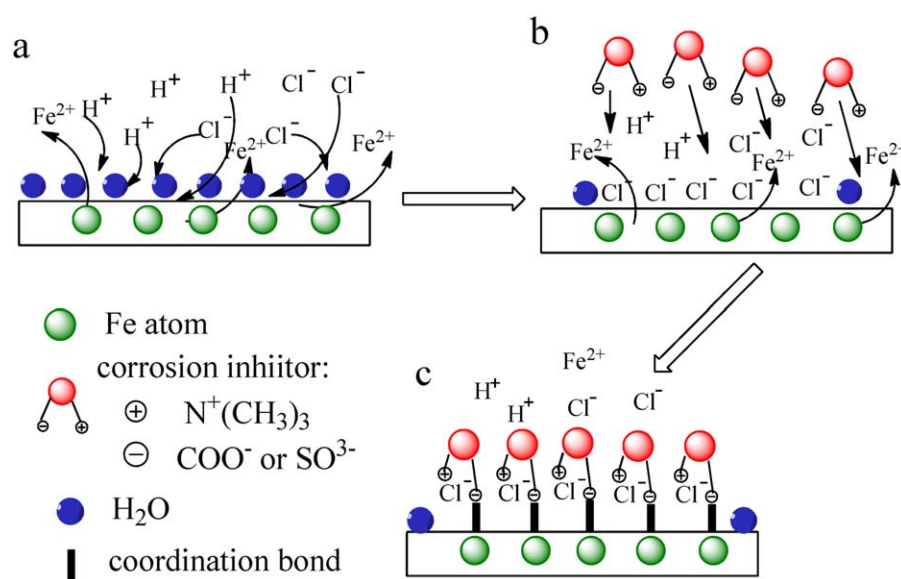
Figure 7. The formation process of the adsorption film. A: Metal in HCl solution; B: Addition of corrosion inhibitor; and C: Adsorption film on the metal. [Color figure can be viewed in the online issue, which is available at wileyonlinelibrary.com.]
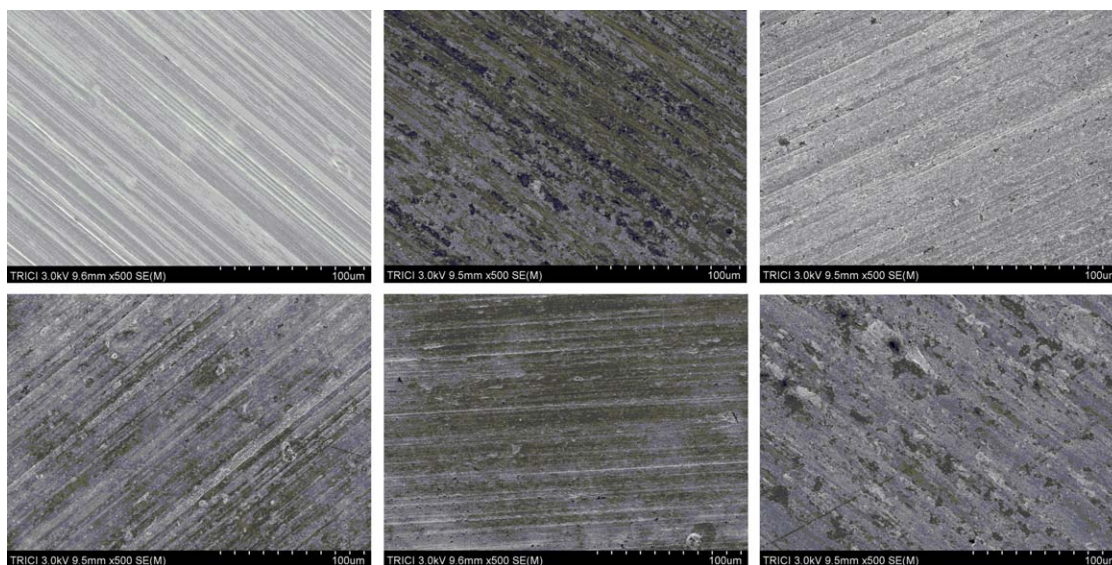
Figure 8. SEM figures of A: uncorroded steel, B: OC (200 mg/L), C: SU-QAOC (100 mg/L), D: PS-QAOC (200 mg/L), E: AMPS-QAOC (100 mg/L), and F: CM-QAOC (100 mg/L). [Color figure can be viewed in the online issue, which is available at wileyonlinelibrary.com.]

dosages. As shown in these figures, it can be seen that the metal surfaces of samples are uneven with some depressions and etching pits. However, the metal surface of OC was more uneven than that of the four OC derivatives. This indicates that the four OC derivatives work well in protecting metal from corrosion. Furthermore, Figure 8B shows that SU-QAOC has much better inhibition effect than the other three derivatives as the surface is smoother than the others.

CONCLUSIONS

The four bi-modified amphoteric OC derivatives have been synthesized and characterized using FT-IR and ^{1}H-NMR spectra. Most of them possessed better antiscaling performances than OC in 1.0 mol/L HCl solution with their own optimal dosages. SU-QAOC and AMPS-QAOC show higher corrosion inhibition efficiencies at a dosage of 100 mg/L than OC at a dosage of 200 mg/L. This is mainly due to their different molecular characters.

The four OC derivatives were found to be hybrid inhibitors with predominating anodic inhibition as characterized using electrochemical polarization, SEM, and EIS measurements. They are all adsorptive corrosion inhibitors. They mainly hinder the charge transfer through adsorbing on the surface of metal and forming complex with metal ions.

For the corrosion inhibitor, better corrosion inhibition efficiency is due to more function groups and stronger coordination ability of function groups. The surface charges, hydrophilicity, polarity, corrosion medium, and volume of function groups may also influence the corrosion inhibition efficiency. More researches should be done on the quantitative analysis of the influence of surface charges, hydrophilicity, polarity, corrosion medium, volume of function groups, and corrosion inhibition efficiency.

REFERENCES

1. Xiao, Y. Y.; Dan, C.; Lian, Y.; Yong, Z. D. *Carbohydr. Polym.* **2011**, *84*, 1357.

2. Jia, Z. S.; Shen, D. F.; Xu, W. L. *Carbohydr. Res.* **2001**, *333*, 1.

3. Fekry, A. M.; Mohamed, R. R. *Electrochim. Acta* **2010**, *55*, 1933.

4. Li, M. L.; Xu, J.; Li, R. H.; Wang, D. E.; Li, T. B.; Yuan, M. S.; Wang, J. Y. *J. Colloid Interface Sci.* **2014**, *417*, 131.

5. Roncal, T.; Oviedo, A.; de Armentia, I. L. *Carbohydr. Res.* **2007**, *342*, 2750.

6. Ma, B.; Zhang, M.; He, C. *J. Carbohydr. Polym.* **2012**, *88*, 347.

7. Yue, W.; Yao, P. J.; Wei, Y. A. *Polym. Degrad. Stab.* **2008**, *93*, 1814.

8. Huang, Q. Z.; Wang, S. M.; Huang, J. F.; Zhuo, L. H.; Guo, Y. C. *Carbohydr. Polym.* **2007**, *68*, 761.

9. Sun, S. L.; Wang, A. Q. *Biochem. Eng. J.* **2007**, *36*, 131.

10. Baumann, H.; Faust, V. *Carbohydr. Res.* **2001**, *331*, 43.

11. Cheng, S.; Chen, S. G.; Liu, T.; Chang, X. T.; Yin, Y. S. *Mater. Lett.* **2007**, *61*, 3276.

12. Sajomsang, W.; Ruktanonchai, U. R.; Gonil, P. *Carbohydr. Polym.* **2010**, *82*, 1143.

13. Alijourani, J.; Raeissi, K.; Golozar, M. A. *Corros. Sci.* **2009**, *51*, 1836.

14. Eduok, U. M.; Umoren, S. A. *Arab. J. Chem.* **2012**, *5*, 325.

15. Bentiss, F.; Traisnel, M.; Lagrenee, M. *Corros. Sci.* **2000**, *42*, 127.

16. Sethuraman, M. G.; Raja, P. B. *Mater. Lett.* **2008**, *62*, 113.

17. Lagrenee, M.; Mernari, B.; Chaibi, N.; Traisnel, M.; Vezin, H.; Bentiss, F. *Corros. Sci.* **2001**, *43*, 951.

18. Arenas, M. A.; Conde, A.; de Damborenea, J. *Corros. Sci.* **2002**, *44*, 511.

19. Zaferani, S. H.; Sharifi, M.; Zaarei, D.; Shishesaz, M. R. *J. Environ. Chem. Eng.* **2013**, *1*, 652.

20. Quraishi, D. A.; Jamal, D. *Mater. Chem. Phys.* **2001**, *68*, 283.

21. Andrea, B.; Alessandro, F.; Vincenzo, G.; Fabrizio, Z. *Corros. Sci.* **2013**, *73*, 80.

22. Deepa, P.; Padmalatha, R. *J. Environ. Chem. Eng.* **2013**, *1*, 676.

23. Zhang, H. X.; Zhu, Y. C.; Wang, F.; Dou, Q.; Wang, D. D. (Hebei University of Technology). China, Patent, CN 10304457 A, April 17, **2013**.

24. Zhang, H. X.; Zhu, Y. C.; Wang, F.; Zhou, H. Y.; Sun, D. X.; Dou, Q. *Chem. Res. Appl.* **2013**, *25*, 377 [in Chinese].

25. Zhang, H. X.; Zhu, Y. C.; Wang, F.; Sun, D. X.; Yang, T. R. (Hebei University of Technology). China, Patent, CN. 103012619. A, April 3, **2013**.

26. Zhang, H. X.; Ge, L. H.; Zhou, H. Y.; Zhu, Y. C.; Wang, F. *Chem. Eng. Prog.* **2011**, *30*, 2055 [in Chinese].

27. Cruz, J.; Martinez, R.; Genesca, J.; Garcia-Ochoa, E. *J. Electroanal. Chem.* **2004**, *566*, 111.

28. Gao, Y. M.; Chen, J. J.; Lei, L. C. *Corros. Sci. Protect. Technol.* **2012**, *22*, 338 [in Chinese].

29. Fuchs-Godec, R.; Miomir, G. *Corros. Sci.* **2012**, *58*, 192.

30. Solmaz, R.; Kardas, G.; Culha, M.; Yazici, B.; Erbil, M. *Electrochim. Acta* **2008**, *53*, 5941.

31. Williams, G.; McMurray, H. N. *Electrochim. Acta* **2012**, *69*, 287.

32. Mayuri, N. K.; Aru, K. J.; Parimal, A. P. *J. Ind. Eng. Chem.* **2013**, *19*, 286.

33. Ghailane, T.; Balkhmima, R. A.; Ghailane, R.; Souizi, A. *Corros. Sci.* **2013**, *76*, 317.

34. Ayse, O. Y.; Gulfeza, K. *Corros. Sci.* **2012**, *58*, 86.

35. Dkhireche, N.; Dahami, A.; Rochdi, A.; Hmimou, J.; Touir, R.; Ebn Touhami, M. *J. Ind. Eng. Chem.* **2013**, *19*, 1996.

36. Behpour, M.; Ghoreishi, S. M.; Khayatkashani, M.; Soltani, N. *Mater. Chem. Phys.* **2013**, *131*, 621.

37. Vedapriya, P.; Stuart, B.; Rolf, G. *Corros. Sci.* **2013**, *72*, 108.

38. Mehdi, M.; Hossein, S.; Azita, K. *Corros. Sci.* **2012**, *65*, 249.

39. Popova, A.; Christov, M.; Raicheva, S.; Sokolova, E. *Corros. Sci.* **2004**, *46*, 1333.

40. Deyab, M. A.; Abd Ei-Rehim, S. S.; Keera, S. T. *Colloid. Surf. A* **2009**, *348*, 170.

41. Khan, A. *Comput. Theor. Chem.* **2014**, *1047*, 67.